Aerosol Science and Technology

ISSN: (Print) (Online) Journal homepage: https://www.tandfonline.com/loi/uast20

Laboratory determination of gravimetric correction factors for real-time area measurements of electronic cigarette aerosols

Sinan Sousan, Jack Pender, Dillon Streuber, Meaghan Haley, Will Shingleton & Eric Soule

To cite this article: Sinan Sousan, Jack Pender, Dillon Streuber, Meaghan Haley, Will Shingleton & Eric Soule (2022) Laboratory determination of gravimetric correction factors for real-time area measurements of electronic cigarette aerosols, Aerosol Science and Technology, 56:6, 517-529, DOI: 10.1080/02786826.2022.2047152

To link to this article: https://doi.org/10.1080/02786826.2022.2047152

AEROSOL SCIENCE AND TECHNOLOGY
2022, VOL. 56, NO. 6, 517–529
https://doi.org/10.1080/02786826.2022.2047152

Laboratory determination of gravimetric correction factors for real-time area measurements of electronic cigarette aerosols

Sinan Sousan[a,b], Jack Pender[c], Dillon Streuber[d], Meaghan Haley[d], Will Shingleton[d], and Eric Soule[d]

[a]Department of Public Health, Brody School of Medicine, East Carolina University, Greenville, North Carolina, USA; [b]North Carolina Agromedicine Institute, Greenville, North Carolina, USA; [c]Department of Chemistry, East Carolina University, Greenville, North Carolina, USA; [d]Department of Health Education and Promotion, College of Health and Human Performance, East Carolina University, Greenville, North Carolina, USA

ABSTRACT

Research on secondhand electronic cigarette (ECIG) aerosol exposure using aerosol monitors has demonstrated that ECIG use can generate high concentrations of particulate matter (PM) and impact indoor air quality. However, quantifying indoor air PM concentrations using real-time optical monitors with on-site calibration specifically for different PM exposures has not been established. Therefore, the ECIG aerosol filter correction factors were calculated for different PM sizes (PM_1, $PM_{2.5}$, and PM_{10}) and different aerosol optical monitors, the MiniWRAS, pDR, and SidePak. ECIG aerosol generation was achieved using five ECIGs representing three ECIG types, disposable, pod-mod, and box mod. The aerosol size distribution by mass was measured for the five ECIGs during PM generation. Compared to the discrete filter measurements, the MiniWRAS performed the best when the concentrations were low, followed by the pDR and SidePak. The average PM concentrations and correction factor ranges for the different ECIGs were 323–1,775 μg/m^3 and 0.64–6.01 for the MiniWRAS, 1,388–13,365 μg/m^3 and 0.41–0.80 for the pDR, and 4,632–55,339 μg/m^3 and 0.13–0.20 for the SidePak, respectively. The mass median diameter ranged from 0.41 to 0.62 μm, and most particles generated from the ECIGs were smaller than 1 μm. This study demonstrates that aerosol size distribution varies between ECIGs. Likewise, the correction factors developed for the real-time aerosol monitors are specific to the ECIG used. Thus, these data can help improve ECIG aerosol exposure measurement accuracy.

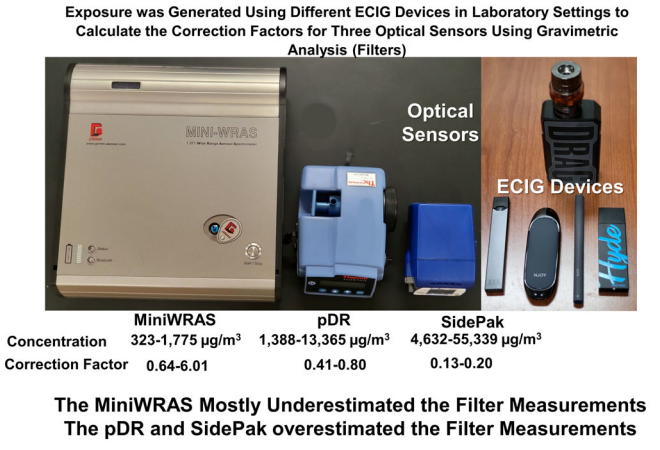

ARTICLE HISTORY
Received 28 October 2021
Accepted 21 February 2022

EDITOR
Mark Swihart

CONTACT Sinan Sousan sousans18@ecu.edu Department of Public Health, Brody School of Medicine, East Carolina University, Carol-Belk Building, 300 Curry Ct, Greenville, NC 27858, USA.

Supplemental data for this article can be accessed at http://doi:10.1080/02786826.2022.2047152.

Introduction

Electronic cigarettes (ECIGs) are devices that use an electric heater to aerosolize a liquid often containing propylene glycol (PG), vegetable glycerol (VG), nicotine, and chemical flavorants (Breland et al. 2017). While ECIGs do not produce smoke through combustion, as in cigarettes or other combustible tobacco products, laboratory research demonstrates that ECIGs generate aerosols that include suspended droplets (i.e. particulate matter or PM) and volatile organic compound vapors. The droplets mainly contain PG, VG, nicotine, water, and flavorings (Czogala et al. 2014; Hutzler et al. 2014; Kosmider et al. 2014; Logue et al. 2017; Schripp et al. 2013; Sleiman et al. 2016; Williams et al. 2017; Williams et al. 2013). Additionally, chemical reactions during ECIG use can generate other toxicants known to be associated with negative health effects, including formaldehyde, acetaldehyde, acrolein, furans, chloropropanols, and tobacco-specific nitrosamines (El-Hage et al. 2019; Flora et al. 2016; Goniewicz et al. 2014; Jensen et al. 2015). Research in exposure chambers (Czogala et al. 2014; Protano et al. 2017; Schober et al. 2014) and real-world settings (Ballbè et al. 2014; Chen et al. 2018; Fernández et al. 2015; Soule et al. 2017; Volesky et al. 2018) have demonstrated that indoor ECIG use can generate high concentrations of PM and greatly impacts indoor air quality. Studies have focused on measuring primary ECIG emissions as well as secondhand and thirdhand ECIG exposure inside laboratory and field settings (Czogala et al. 2014; Goniewicz and Lee 2015; Hiler et al. 2020). These studies measure ECIG aerosol area exposure inside a controlled laboratory chamber.

Recent data suggest exposure to secondhand ECIG aerosol (i.e. bystanders' exposure to ECIG-generated aerosol) may be associated with negative health effects. Visser et al. (2019) reported that secondhand ECIG aerosol contains toxicants including nicotine, PG, copper, and tobacco-specific nitrosamines. *In-vitro* data show that primary emissions and secondhand aerosols can impact cell metabolism and oxidative stress in epithelial cells (Jarrell et al. 2021). Carwile et al. (2019) reported that prevalence of asthma among children was higher in houses where adults reported indoor ECIG use based on data from a study conducted between 2016 and 2017 in the United States. In addition, Gentzke et al. (2019) reported that more than 50% of adolescents in the United States are exposed to secondhand cigarette aerosol and ECIGs aerosol regularly. ECIGs exposure and their related health effects are new, and unfortunately, the long-term health effects of firsthand and secondhand exposures will not be known for a long period. Exposure to ECIG aerosol is particularly of concern due to the size of particles that are inhaled and could have detrimental health effects.

ECIGs generate $PM_{2.5}$ (PM 2.5 µm and smaller in diameter) and are particularly dangerous because they penetrate and deposit deeper into the lungs and could reach the alveoli, where air exchanges occur with the blood and translocate to other organs of the body (Choi et al. 2010; Hinds 1999). The Environmental Protection Agency (EPA) and World Health Organization (WHO) list $PM_{2.5}$ and PM_{10} (PM 10 μm and smaller in diameter) as environmental hazards, and $PM_{2.5}$ as an indoor hazard (EPA. 1990; EPA 2021; WHO. 2010; 2018). EPA and WHO have no indoor regulations for $PM_{2.5}$ and PM_{10}. However, the WHO has concluded that there is no difference in the hazardous nature of $PM_{2.5}$ and PM_{10} between indoor and outdoor settings (WHO. 2018). In addition, there is an increasing interest in PM_1 (particles 1 µm and smaller in size) particles due to their short-term effects, increased morbidity and mortality, and cardiopulmonary effects (Bari et al. 2015; Chen et al. 2017; Wang et al. 2021a; Wang et al. 2021b). Environmental effects are based on indirect PM sources and inhaling PM directly can have a more severe effect. In addition, bystanders of ECIG user may be exposed to the compounds common to ECIG aerosols that are known to cause negative impacts on health through secondhand exposure (David et al. 2020; Logue et al. 2017; McGrath-Morrow et al. 2020). Due to the potential for negative health effects from exposure to secondhand ECIG aerosol, ECIG-generated PM concentrations are often measured using discrete and real-time monitors.

PM measurements are obtained using gravimetric analysis, which is considered the gold standard for air quality monitoring (Sousan, Regmi, and Park 2021). The method uses filter samples to calculate time-weighted average (TWA) PM mass concentration by weighing the mass difference of PM accumulated on the filter at a specific flow rate and sampling time (Olegario, Regmi, and Sousan 2021). However, gravimetric analysis is time-consuming and requires specialized laboratories to control the temperature within ±1 °C and relative humidity between 30% and 50% with ± 5% variability (Hinds 1999). In addition, gravimetric analysis provides an average concentration value over the sampling time with no temporal information. On the other hand, light scattering monitors provide real-time PM mass concentration and are inexpensive to operate (Sousan et al. 2016b). Optical particle counters (OPCs) use the magnitude of light scattered from particles to count the number of particles per size (e.g. $PM_{2.5}$) and calculate the mass

Table 1. Settings for different E-CIG devices.

	Flow (L/min)	Puffs (ON/OFF) [seconds]	Experiment Runtime [minutes]	Liquid Ratio of ECIG (P.G./V.G.)	Power (W)	Heater Resistance (Ω)	Voltage (V)
VooPoo Drag 2	8.5	4/30	15	35/65	70[a]	0.23	7.5[a]
JUUL	1.5	5/30	60	27/73[2]	0.62–4.08[b]	1.83[b]	1.13–2.72[b]
NJOY Ace	1.0	4/30	30	NA[3]	NA[c]	NA[c]	NA[c]
NJOY Daily	1.0	4/30	30	NA[3]	NA[c]	NA[c]	NA[c]
Hyde	1.0-1.5	4/30	30	19/81[4]	8.28[d]	1.75[d]	3.81[d]

[a]Displayed on the device (not measured).
[b]Talih et al. (2020).
[c]NA: Not Available in the literature or the manufacturer's website.
[d]Talih et al. (2021).

concentration at different PM sizes. Photometers use light scattering from an assembly of particles passing at a specific angle to estimate mass concentration at a specific PM size based on a linear regression model. However, these devices require on-site filter correction as recommended by the manufacturer (GRIMM. 2010; Sousan et al. 2016a; ThermoFisherScientific 2010). Multiple field and laboratory studies have measured ECIG $PM_{2.5}$ concentrations in ECIGs discussed in the next paragraph.

Field studies have measured $PM_{2.5}$ concentrations in indoor settings with active ECIG users using different aerosol monitors without filter correction. Schober et al. (2019) measured $PM_{2.5}$ inside vehicles using the Grimm 1.108 OPC and a Grimm NanoCheck 1.320 to cover the entire particle size range and reported real-time concentrations up to ~6,000 μg/m^3. Melstrom et al. (2017) measured $PM_{2.5}$ inside a 52.6 m^3 room using a SidePak photometer and a TSI P-Trak to examine the entire particle size range and reported concentrations up to ~19,000 μg/m^3. Volesky et al. (2018) measured $PM_{2.5}$ inside a 38 m^3 office using a TSI DustTrak photometer at 0.5 and 1 m away from the participant and reported 289.5 and 246.9 μg/m^3 mass concentrations, respectively. In contrast, Czogala et al. (2014) measured $PM_{2.5}$ concentrations from machine-generated ECIG aerosol inside a 39 m^3 chamber in laboratory settings using a SidePak and a filter calibration factor of 0.32 that has been used previously to examine cigarette smoke PM concentrations. This study reported $PM_{2.5}$ concentrations up to ~1,000 μg/m^3. However, cigarette smoke and ECIG aerosol have different aerosol size distributions, due to different aerosol mechanisms of generations, differences in refractive index between solid and liquid aerosols, and particle shape. Therefore, there is a need to identify new correction factors for ECIG aerosol.

The objective of this study was to calculate filter correction factor values for different ECIG devices and different PM optical monitors. In addition, this study will provide considerations for researchers looking to measure aerosol concentrations for future studies using different real-time aerosol monitors. First, the filter correction factors were calculated for different particle sizes of three real-time monitors for five different ECIGs: one box mod (VooPoo Drag 2), two pod mods (JUUL, 5% nicotine concentration label and NJOY Ace), and two disposable ECIG devices (NJOY Daily and Hyde). Then, the aerosol size distributions of the five different ECIGs were measured.

Material and methods

Five ECIGs were used to generate PM inside an airborne-controlled laboratory chamber to measure PM_1, $PM_{2.5}$, and PM_{10}. Measurements were performed with discrete gravimetric analysis to measure the reference and real-time optical monitors to capture temporal variability. Finally, the equipment used in this section to achieve the required measurements will be described.

Real-time reference monitors

MiniWRAS real-time monitor

The specifications of the real-time equipment used in the study are listed in Table S1 in the supplemental information. The GRIMM Mini Wide-Range Aerosol Spectrometer (MiniWRAS 1371, Grimm Aerosol Technik, Ainring, Germany) is a high-cost (>$30,000) real-time monitor that measures PM in a wide particle size range between 0.01 μm and 35 μm in 41 number count bin sizes. The device was chosen because it can measure the entire size range of PM and calculate PM_1, $PM_{2.5}$, and PM_{10}, which was required for this study. The device uses two technologies to examine this size range: an optical monitor for particles larger than 0.25 μm and a corona charger to measure particles 0.25 μm and smaller. The MiniWRAS uses different laser powers to detect particles smaller than 2.5 μm, compared to larger particles, to achieve reliable estimates for these smaller sizes (Sousan, Regmi, and Park 2021). The device samples air at a flow rate of 1.2 L/min and measures PM mass concentration between 0-

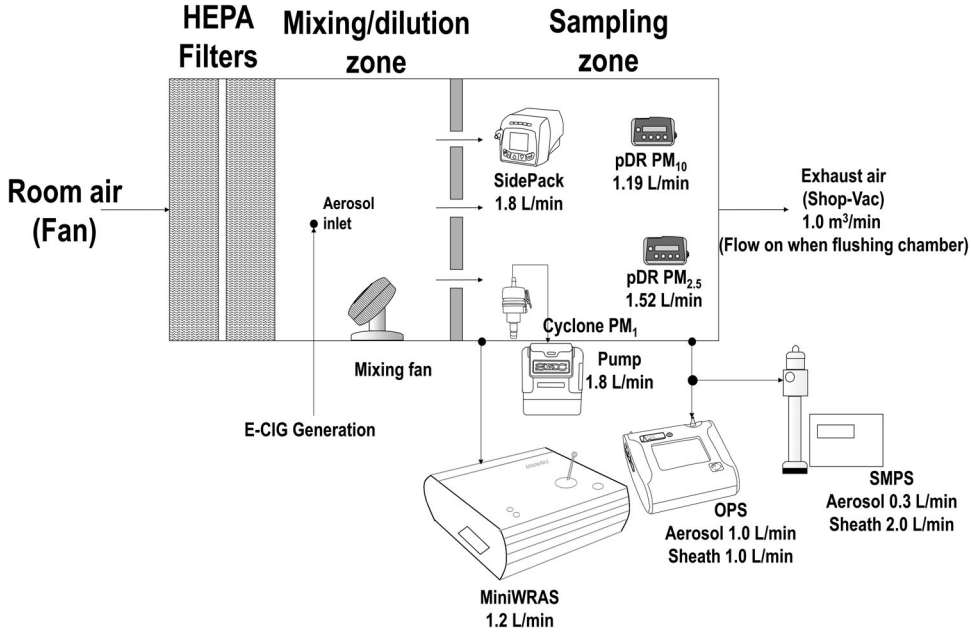

Figure 1. Experimental setup used to measure E-CIG exposure of Different Vaping Devices.

100,000 $\mu g/m^3$. The MiniWRAS is an evolved Grimm 1.108 OPC modified to measure particles smaller than 0.25 μm that cannot be detected with optical science. The MiniWRAS was set to record data with a 1-minute frequency.

pDR 1500 real-time monitor

The personal DataRAM (pDR 1500, Thermo Scientific, Franklin, MA, USA) is a medium-cost (~$7,000) real-time photometer that measures PM at a specific size using a cyclone operated at a specific flow rate. The device was chosen because it is equipped with a built-in 37 mm filter holder that can be used to collect PM for gravimetric analysis. The device measures PM mass concentration between 0 and 400,000 $\mu g/m^3$. Two pDRs were used for this study to measure $PM_{2.5}$ and PM_{10}, equipped with 2.5 and 10 μm (50% cut-point) cyclones and flow rates of 1.52 and 1.19 L/min, respectively. The pDRs were set to record data with a 1-second frequency.

SidePak real-time monitor

The SidePak Personal aerosol monitor (AM520, TSI Inc., Shoreview, MN, USA) is a medium-cost (~$5,000) real-time photometer that measures PM at a specific size using an impactor. The device was chosen due to its relatively lower cost and greater usage among the ECIG and cigarette researcher community (Czogala et al. 2014; Jiang et al. 2011; Klepeis, Ott, and Switzer 2007; Melstrom et al. 2017). The device samples air at a flow rate of 1.8 L/min and measures PM mass concentration between 0 and 100,000 $\mu g/m^3$. The SidePak was used to measure $PM_{2.5}$ equipped with a 2.5 μm (50% cut-point) impactor. The SidePak was set to record data with a 1-second frequency.

Discrete PM measurement

An SCC 0.695 cyclone (BGI, INC, Waltham, MA, USA) was used to measure PM_1. The SCC 0.695 cyclone was operated with an SKC AirChek TOUCH (SKC Inc., Cat. No. 220-5000TC, Eighty Four, PA, USA) air sampling pump at a flow rate of 1.8 L/m. The cyclone and pump were calibrated daily using a calibration shroud (BGI, Item number: 188303, Waltham, MA, USA) and chek-mate calibrator (SKC Inc., Cat. No. 375-0550 N, Eighty Four, PA, USA).

Gravimetric analysis

The pDRs and the discrete PM method were equipped with a 37 mm fiberglass filter (Whatman, CAT Non.1827-037, Maidstone, United Kingdom) to collect mass for gravimetric analysis. The filters were pre- and post-weighed using a Mettler Toledo microbalance (Model: XPR6UD5, Columbus, Ohio, USA) and an anti-static kit with a large U-electrode (Model: 63052302, Mettler Toledo, Columbus, Ohio, USA). The filter mass concentration was calculated by dividing the difference between the filter mass pre- and post-weight with the flow rate and sampling time. In addition, the filters were equilibrated for temperature and relative humidity inside the balance room at

Table 2. Correction factors for instruments of each particle size and ECIG device. The average and standard deviation were computed based on three experiments.

PM Sensor-Size	Average	Standard Deviation
(A) VooPoo Drag 2		
MiniWRAS PM1	3.99	2.05
MiniWRAS PM2.5	6.01	0.27
MiniWRAS PM10	5.48	0.32
pDR PM2.5	0.80	0.08
pDR PM10	0.69	0.04
SidePak PM2.5	0.18	0.01
(b) *JUUL*		
MiniWRAS PM1	1.72	0.11
MiniWRAS PM2.5	1.90	0.46
MiniWRAS PM10	2.05	0.60
pDR PM2.5	0.59	0.10
pDR PM10	0.59	0.14
SidePak PM2.5	0.13	0.02
(C) NJOY Ace		
MiniWRAS CF PM1	2.15	0.53
MiniWRAS CF PM2.5	2.66	0.36
MiniWRAS CF PM10	2.56	0.26
pDR CF PM2.5	0.67	0.08
pDR CF PM10	0.62	0.10
SidePak CF PM2.5	0.19	0.02
(d) *NJOY Daily*		
MiniWRAS PM1	1.42	0.46
MiniWRAS PM2.5	2.52	0.78
MiniWRAS PM10	2.28	0.63
pDR PM2.5	0.68	0.07
pDR PM10	0.58	0.07
SidePak PM2.5	0.18	0.01
(e) *Hyde*		
MiniWRAS PM1	0.64	0.11
MiniWRAS PM2.5	1.38	0.24
MiniWRAS PM10	1.30	0.14
pDR PM2.5	0.45	0.09
pDR PM10	0.41	0.03
SidePak PM2.5	0.20	0.06

$22 \pm 1\,^{\circ}C$ and between $45 \pm 5\%$, respectively (Hinds 1999).

Experimental setup

Chamber description

Experiments were conducted inside the Research Aerosol Laboratory located at East Carolina University. The laboratory contains an airtight $0.5\,m^3$ exposure chamber used for controlled aerosol generation and assessment, as shown in Figure 1. The chamber was split in half, where the first half represented the mixing zone ($0.25\,m^3$ in size) and the other half the sampling zone ($0.25\,m^3$ in size). Particle-free air was supplied at a flowrate of $1.00\,m^3$/min to the mixing zone using two (HEPA) filters with 99.99% efficiency. The chamber was flushed with particle-free air between experiments (Sousan, Regmi, and Park 2021). Air was removed from the chamber using a vacuum that included two HEPA filters for aerosol removal and a carbon filter for gas removal. During the experiments, the inlet dilution air to the chamber and vacuum was turned off to increase the mass concentration inside the sampling zone. This was done as *dilution* air prevented the filters from achieving the limit of detection. A honeycomb flow straightening section separated the two zones (AS100, Ruskin, Grandview, MO, USA) used to create an even distribution in the sampling zone by mixing the air with two fans, operated at a flow rate of $0.20\,m^3$/min in the mixing zone. The fans were operated during the experiment and when the chamber was flushed with dilution air in between experiments. The aerosol homogeneity of the sampling zone was tested before the experiment by placing four real-time optical aerosol monitors in the middle and sides of the zone while measuring salt aerosol concentration, and the average differences were ~9% for both positions. The pDR, SidePak, and SCC 0.695 cyclone were positioned in the sampling zone of the chamber. The MiniWRAS was positioned outside the chamber and sampled air directly from the sampling zone using an isokinetic tube. The AirChek TOUCH pump was positioned outside the chamber and was attached to the cyclone with a tube. Temperature and relative humidity inside the chamber were maintained at $22 \pm 2\,^{\circ}C$ and $45 \pm 5\%$, respectively.

Aerosol generation

The ECIGs used in the current study are shown in Table S2 in the supplemental information. Five ECIGs readily available in the market were used in this study that included a "box mod" device (VOOPOO DRAG 2; (VAPING. 2021)), two "pod mod devices" (JUUL (JUUL. 2021)); NJOY Ace (NJOY. 2021), and two disposable ECIG devices (NJOY Daily (NJOY. 2021); Hyde Original (Hyde 2021)). The VooPoo Drag 2 has a refillable tank loaded with Hawaiian POG flavored liquid (30/70 propylene glycol/vegetable glycerin ratio, 3 mg/ml nicotine concentration) liquid (PerfectVap 2021). During the experiments, a UFLORCE U4 (0.23 Ω) coil was used and the device was set to operate at a default wattage of 70 W. The JUUL and NJOY Ace have replaceable pods, and the Hyde and NJOY Daily are disposable products. Aerosols were generated using a diaphragm pump (Thomas 1420-0504, Gardner Denver, Davidson, NC, USA), and a clock generator (TFIS 12-240VUC 1CO CG, Weidmüller Interface GmbH & Co. K.G., Detmold, Germany). The clock generator was used to control the ECIG puffing time. The pump generated 4 s puffs with an interpuff interval of 30 s, similar to puffing data reported from ECIG users (Hiler et al. 2020). The diaphragm pump flow rate differed between the ECIGs

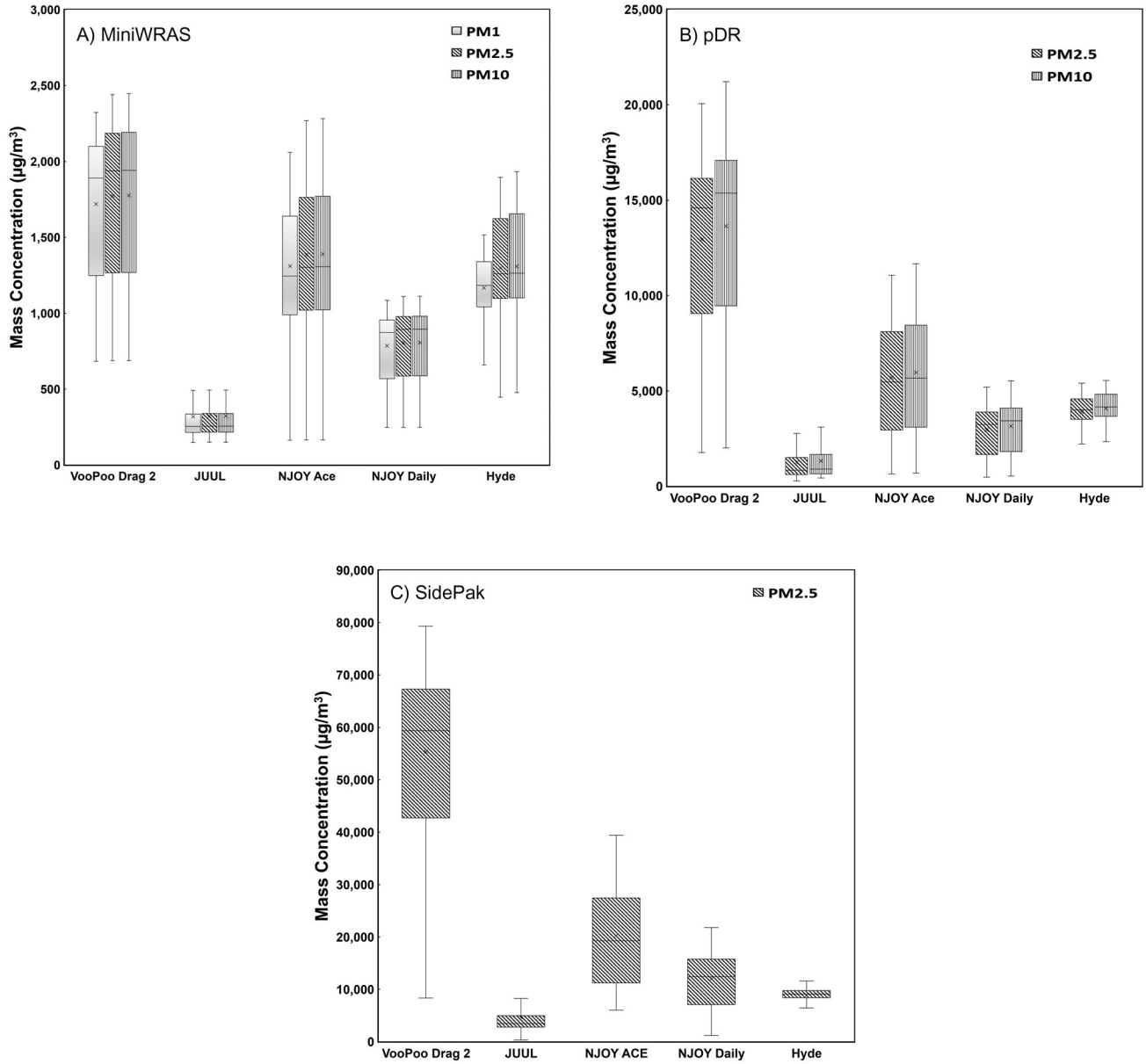

Figure 2. Size-selective Box-Whisker plots for (a) MiniWRAS, (b) pDR, and (c) SidePak. The MiniWRAS measures PM1, PM2.5, and PM10, whereas two pDRs were used, one for PM2.5 and the other for PM10 measurements, and the SidePak only measured PM2.5. The measurements represent non-filter-corrected raw data.

with 1–1.5 L/m for the pod mods and disposable devices (Vargas-Rivera et al. 2021) and 8.5 L/m for the VooPoo Drag 2 (Hiler et al. 2020). The experiments were repeated three times with each ECIGs.

Data analysis

Real-Time mass concentrations

PM concentrations measured from the pDRs and the SidePak were averaged over 1 min and paired with the MiniWRAS, which was collected for 1 min. Box and Whisker plots of each sensor, MiniWRAS, pDR, and SidePak were plotted for PM_1, $PM_{2.5}$, and PM_{10}. PM concentrations measured by particle size were PM_1, $PM_{2.5}$ and PM_{10} from the MiniWRAS, PM_1 and $PM_{2.5}$ from the pDR, and $PM_{2.5}$ from the SidePak.

Filter correction factors

Filter correction factors were calculated for each PM monitor, particle size, and ECIG device by dividing the discrete filter mass concentration by the average real-time mass concentration measured by the PM monitors.

Aerosol size distribution

The aerosol size distribution by mass was captured with multiple devices in separate experiments listed in the previous sections. The first device was the

MiniWRAS that captures the distribution in 41 bins. To compare the MiniWRAS measurements, a high-cost reference instrument, the Scanning Mobility Particle Sizer Spectrometer (SMPS 3938, ~$91,000, TSI, Shoreview, Minnesota, USA) coupled with the Optical Particle Sizer (OPS 3330, ~$16,000, TSI, Shoreview, Minnesota, USA) were used. The SMPS has 191 bins measuring particle size using electrical mobility, compared to the MiniWRAS, which has 41 bins, 10 electrical and 31 optical. The optical science measures the remaining bin sizes. The SMPS system includes a 3082 electrostatic classifier, 3081 A Long Differential Mobility Analyzer, 3756 Ultrafine Condensation Particle Counter, and an advanced aerosol soft Xray neutralizer. The SMPS was operated at an aerosol and sheath flows of 0.3 L/min and 2 L/min, respectively. The SMPS uses electric mobility to measure submicron particles between 0.001 and 1.0 µm. The SMPS was operated with a 0.0508 cm impactor and a 50% cut-point of 0.72 µm. Therefore, the OPS that incorporates optical science to capture the number size distribution between 0.3 and 10 μm in up to 16 channels was used. The OPS operates at an aerosol and sheath flow of 1.0 L/min each. The SMPS and OPS were positioned outside the chamber while sampling air directly from the sampling zone in Figure 1. The SMPS and OPS were set to record data with a 1-minute frequency. The SMPS and OPS were used once with the MiniWRAS for each ECIG generation method, except for the NJOY Ace, where only the SMPS and MiniWRAS were available at the time of the experiment. Therefore, the SMPS + OPS data for the NJOY Ace measurements were not provided.

TSI provides the Multi-Instrument Manager (MIM) software (version 3.0) to perform the SMPS and OPS data curve fitting using a lognormal distribution function. The default automated curve fitting options were used for these calculations. The mass median diameter (MMD) and geometric standard deviation (GSD) were tabulated for the MiniWRAS, SMPS, OPS, and the curve fitted data. The aerosol size distribution for MiniWRAS and the SMPS + OPS fitted data were plotted for each ECIG generation method. Particle size was converted to volumetric particle diameter for all monitors. PG and VG, once aerosolized, generate liquid particles, and those aerosol particles are spherical in shape. Therefore, this study assumed the shape factor as 1 for all aerosol generated from different ECIG types (Hinds 1999). The density was assumed as 1.16 g/ml, based on a one-to-one ratio of P.G. (1.04 g/ml) and V.G. (1.27 g/ml) (Sleiman et al. 2016).

Results and discussion

The diaphragm pump flow rates, the clock generator vaping time for the ECIGs, and experiment times for this study are listed in Table 1. The disposables and the pods were set to operate at 1 L/m, however, measurable PM with the JUUL and two of the Hyde experiments at that desired flow could not be achieved, so the flow rate was increased to 1.5 L/m. As a result, the generation time for each ECIG was 15 min for VooPoo Drag 2 and 30 min for NJOY Ace, NJOY Daily, and Hyde. The JUUL experiments deviated from the other ECIG generation methods, where the puffing time of 5 s and generation of 60 min was chosen because the filter limit of detection at 4-second puffs and 30-minute generation time was not achieved. In addition, all the JUUL pods were used for 30 min before the experiments, where new pods did not generate sufficient mass on the filters to exceed the limit of detection. In contrast, 15 min and 4 puffs were sufficient for the VooPoo Drag 2 to exceed the filter limit of detection.

Real-Time mass concentrations

The non-filter-corrected raw real-time data for the MiniWRAS, pDR, and SidePak with their respective particle sizes measured during the experiments are shown in Figure 2. The PM monitors reported different concentrations between devices and for each ECIG generation method. The average $PM_{2.5}$ concentrations as measured by the MiniWRAS were as follows: VooPoo Drag 2 (1,775 µg/m^3), JUUL (323 µg/m^3), NJOY Ace (1,389 µg/m^3), NJOY Daily (806 µg/m^3) and Hyde (1,309 µg/m^3); as measured by the pDR were as follows: VooPoo Drag 2 (13,365 µg/m^3), JUUL (1,388 µg/m^3), NJOY Ace (5,966 µg/m^3), NJOY Daily (3,157 µg/m^3), and Hyde (4,086 µg/m^3); and as measured by the SidePak were as follows: VooPoo Drag 2 (55,339 µg/m^3), JUUL (4,632 µg/m^3), NJOY Ace (20,254 µg/m^3), NJOY Daily (12,028 µg/m^3) and Hyde (8,846 µg/m^3). The lowest measurements for the ECIGs were for the PM_1 JUUL concentrations as follows: MiniWRAS (148 µg/m^3), pDR (289 µg/m^3), and SidePak (340 µg/m^3), and the highest measurements were for the PM_{10} VooPoo Drag 2 concentrations as follows: (2,446 µg/m^3), (21,213 µg/m^3), (79,310 µg/m^3).

The VooPoo Drag 2 ECIG generated the highest PM concentrations in all sizes and the JUUL generated the lowest concentrations. The SidePak monitor reported the highest average $PM_{2.5}$ concentrations with values 31 and 4 times higher than the MiniWRAS and pDR, respectively, when compared

using the VooPoo Drag 2. The average $PM_{2.5}$ and PM_{10} measurements within the same monitor were comparable for the MiniWRAS and pDR measurements for all ECIG generation methods. For the MiniWRAS PM_1 average measurements, the values were similar to the $PM_{2.5}$ and PM_{10}, except for differences for the Hyde generation of 126 $\mu g/m^3$. The $PM_{2.5}$ average concentrations for the pDR indicated that values were mostly smaller than 2.5 µm for all ECIGs. In contrast, the MiniWRAS PM_1 concentrations indicated that values were mostly below 1 µm for all ECIGs, especially for Hyde, indicating PM_1 and $PM_{2.5}$ concentrations were not the same. The high concentrations exhibited by the VooPoo Drag 2 were most likely due to the high wattage utilized by the device which resulted in more ECIG liquid being aerosolized. In contrast, the wattages of the disposables or the JUUL were not measured, but the JUUL (Talih et al. 2020), and other disposable vapes (Talih et al. 2021) operate at lower wattage. Previous research has shown that high device wattage is associated with greater particulate matter production (Talih et al. 2017).

Aerosol light scattering instruments are valuable tools used to estimate real-time mass concentration (Hinds 1999). However, light scattering is sensitive to different parameters such as refractive index, scattering angle, particle size and particle shape. In addition, these monitors are usually manufactured with default parameters representing ideal laboratory conditions. Therefore, aerosol monitor manufacturers recommend creating an onsite filter calibration factor using gravimetric analysis to correct the real-time measurements (GRIMM. 2010; ThermoFisherScientific 2010). Studies have also used refractive index correction to the intensity of light measured using these real-time monitors (Ingebrethsen, Cole, and Alderman 2012; Liu and Daum 2000; Rosenberg et al. 2012). The current work uses gravimetric analysis to correct light scattering disadvantages as recommended by instrument manufacturers and adopted by different studies (Burkart et al. 2010; Czogala et al. 2014; Sousan, Regmi, and Park 2021; Wang et al. 2016). The data presented in Figure 2 represent the raw real-time mass concentrations biased due to differences in light scattering parameters. However, the data can be corrected using the filter correction factors developed in the next section. Therefore, the next paragraph compares raw data from this work with raw real-time data from previous studies.

While other studies focus on $PM_{2.5}$, the current study also examined PM_1 and PM_{10}. Schober et al. (2019) examined secondhand ECIG exposure inside vehicles and measured $PM_{2.5}$ using the Grimm 1.108 OPC. Participants in this study used an ECIG inside of a vehicle taking 4-second puffs. The researchers reported an average $PM_{2.5}$ range of 8-490 $\mu g/m^3$ between vehicles. In comparison, in this study, the average $PM_{2.5}$ concentration measured by the MiniWRAS for the NJOY and JUUL experiments were 804 and 321 $\mu g/m^3$, respectively, with higher values for the VooPoo Drag 2 and Hyde. Melstrom et al. (2017) performed secondhand ECIG exposure inside a ~53 m^3 room and measured $PM_{2.5}$ using a SidePak. The participants used a disposable and tank-style ECIG, and the study reported $PM_{2.5}$ concentrations up to 19,961 and 19,972 $\mu g/m^3$, respectively, for both devices. Similarly, the SidePak in the current study reported up to 21,800 $\mu g/m^3$ $PM_{2.5}$ concentration. However, this study did not use participants to generate ECIG secondhand aerosol. Rather a diaphragm pump was used to simulate aerosol vaping at the same flow rates provided from the literature. Therefore, these results might differ if participants are recruited to vape inside the chamber.

Filter correction factors

The filter correction factors and standard deviation of the MiniWRAS, pDR, and SidePak for each particle size and ECIG are shown in Table 2. The correction factors were different between devices. A correction factor of 1.0 indicates that the average real-time concentration of the optical monitor is equal to the discrete filter measurement. A correction factor above unity or below unity indicates that the monitor underestimates or overestimates the discrete filter measurement, respectively. The correction factor range between ECIGs and particles sizes was 0.64-6.01 for the MiniWRAS, 0.41-0.80 for the pDR, and 0.13-0.20 for the SidePak. In general, the MiniWRAS underestimated the true mass (filter) concentration for all particle sizes and ECIGs, except for the Hyde PM_1 concentrations. The lowest underestimation was with the Hyde ECIGs, where values were within ±40% around unity, and the highest underestimation was with VooPoo Drag 2 with values up to 500% above unity (1.0). The pDR and SidePak both overestimated all particle sizes, but the SidePak exceeded the pDR values. The pDR overestimation was variable with 20% and 60% below unity for the VooPoo Drag 2 and Hyde, respectively. The SidePak underestimation was consistent with an ≥80% value below unity. In comparison between particle sizes for the same monitor,

Table 3. The MMD and GSD for each E-CIG device based on the SMPS, OPS, and SMPS + OPS fitted data. The average and standard deviation (between brackets) were computed based on three measurements.

	SMPS		OPS		SMPS + OPS (Fitted Data)		MiniWRAS	
Device	MMD (μm)	GSD	MMD (μm)	GSD	MMD (μm)	GSD	MMD (μm)	GSD
VooPoo Drag 2	0.22(0.01)	2.5	0.40(0.01)	1.5	0.43(0.01)	1.2	0.40(0.02)	1.4
JUUL	0.25(0.01)	2.0	0.37(0.01)	1.5	0.41(0.01)	1.2	0.37(0.01)	2.2
NJOY Ace	0.22(0.02)	2.1	–	–	–	–	0.47(0.01)	1.5
NJOY Daily	0.23(0.01)	2.2	0.42(0.01)	1.5	0.46(0.01)	1.4	0.39(0.01)	1.8
Hyde	0.28(0.01)	2.0	0.50(0.01)	1.5	0.62(0.01)	1.6	0.50(0.02)	1.9

the MiniWRAS and pDR have similar correction factors for $PM_{2.5}$ and PM_{10}, but the MiniWRAS PM_1 values were lower than $PM_{2.5}$ and PM_{10} for all ECIG generation methods. The MiniWRAS high underestimation values for the VooPoo Drag 2 are because the device does not handle high concentrations for particles 0.25 μm and smaller. Instead, the manufacturer recommends an aerosol diluter that could cost up to $5,000 if purchased from Grimm. The pDR performed better than the SidePak because the manufacturer calibrates the former to operate with four times higher mass concentrations than the SidePak.

In comparison with this study, Czogala et al. (2014) performed ECIG aerosol exposure inside a 39 m^3 chamber and measured $PM_{2.5}$ using the SidePak AM510 while applying a correction factor of 0.32. The correction factor used in the study was based on previous studies investigating regular cigarettes with the SidePak. ECIG exposure was generated using a vaping machine with a duration of 1.8 s ON and 10 s OFF for 1 h using three ECIG popular brands sold in Poland. The researchers reported $PM_{2.5}$ concentrations up to 1,000 $\mu g/m^3$. The correction factors calculated for this study for the SidePak were between 0.13 and 0.2 for different ECIGs, and the maximum concentration reached by the filter corrected JUUL $PM_{2.5}$ concentration was 1,074 $\mu g/m^3$. The slight difference between the correction factors could be attributed to the type of exposure, ECIG compared to regular cigarettes and the SidePak models, where the SidePak AM520 model was used in this study. Therefore, SidePak has a higher correction for ECIGs compared to regular cigarettes, and all monitors have different correction factors depending on the ECIG used.

Aerosol size distribution

The MMD, volumetric diameter, and GSD values for the SMPS, OPS, SMPS + OPS fitted data, and MiniWRAS are shown in Table 3. In addition, the aerosol size distribution by mass for the SMPS + OPS fitted data and MiniWRAS are shown in Figure 3. The MMD range between ECIGs was 0.22-0.28 μm for the SMPS, 0.41-0.62 μm for the SMPS + OPS, and 0.37-0.5 μm for the MiniWRAS. The SMPS captured MMD values with an average of 0.24 ± 0.03 μm for all ECIG generation types. However, the SMPS was only set to measure particles smaller than 0.72 μm. Therefore, the SMPS + OPS fitted data were a better comparison with the MiniWRAS. The MMD values for the SMPS + OPS fitted data and the MiniWRAS were similar for the VooPoo Drag 2, JUUL, and NJOY Daily, with differences between 0.03 and 0.07 μm. In contrast, for the Hyde ECIG generation, the SMPS + OPS fitted data MMD value was slightly higher at 0.62 μm, compared to 0.5 μm for the MiniWRAS. In addition, the SMPS + OPS aerosol size distribution for VooPoo Drag 2, NJOY, and JUUL shows the particles are smaller than 1 μm for both datasets. In contrast, Hyde's SMPS + OPS aerosol size distribution shows that some particles are larger than 1 μm but smaller than 2.5 μm. These results align well with Figure 2-A, MiniWRAS results, where $PM_{2.5}$ and PM_{10} concentrations are higher than PM1 for Hyde ECIG generation, but PM1, $PM_{2.5,}$ and PM_{10} concentrations are similar for VooPoo Drag 2, NJOY, and JUUL. The slight difference between the SMPS + OPS fitted data and the MiniWRAS for the Hyde aerosol size distribution and MMD could be attributed to the automated settings for the MIM software that can be changed. Finally, it is important to mention that the aerosol size distribution data provided in Table 3 and Figure 3 does not take into account the refractive index differences between ECIG types for the OPS and the larger bins (≥0.25 μm) of the MiniWRAS (Ingebrethsen, Cole, and Alderman 2012). In addition, studies have shown that the dilution factor used in electrical mobility monitors to estimate particle size cause P.G. and V.G. evaporation and shifts the aerosol size distribution to smaller particle sizes for the SMPS and smaller bins (<0.25 μm) of the MiniWRAS (Kane and Li 2021).

In comparison with this study, Sundahl, Berg, and Svensson (2017) measured MMD, aerodynamic diameter, using a Next Generation Pharmaceutical Impactor (NGI) and a custom-made aerosol generation for 13 popular ECIG brands sold in the United Kingdom. The NGI reported different MMD values between 0.53 and 0.96 μm. The MMD values measured for this study were lower between 0.41 and 0.62. However, the volumetric

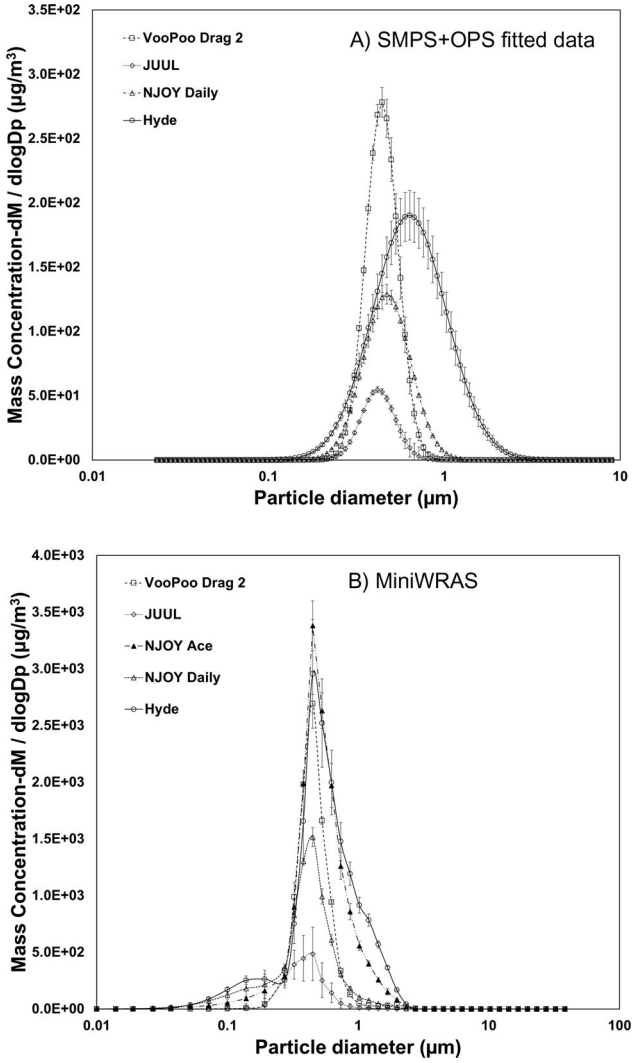

Figure 3. Aerosol size distribution by mass for the (a) SMPS + OPS fitted data and (b) MiniWRAS for the different ECIG devices. The x-axis represents the volumetric particle diameter. Each curve's average and standard deviation were computed based on three measurements. The y-axis represents the standard deviation of the three measurements.

diameter was reported compared to the aerodynamic diameter presented by Sundahl, Berg, and Svensson (2017). When converted from the volumetric diameter, the aerodynamic diameter has a higher value (Peters et al. 1993). Therefore, MMD values for both studies are comparable.

Filter correction factors are crucial for real-time PM monitors, where aerosol manufacturers recommend on-site calibration with gravimetric analysis to increase the accuracy of the measurements (Sousan et al. 2018). This study calculated filter correction factors for ECIG aerosol exposure of three PM monitors, the MiniWRAS, pDR, and SidePak, for five mainstream ECIGs and different particle sizes. The correction factors were measured in an exposure chamber using a diaphragm pump. Real-life scenarios with participants vaping could yield different results. Therefore, researchers should use the filter correction factors calculated from this study with caution in real-life scenarios. Future work should be performed to compare these results with real-life scenarios.

Conclusion

This study shows that correction factors must be developed for different ECIGs and different optical monitors. In addition, this study shows that the ECIG particles were smaller than 1 μm for most PM generated from the ECIGs examined. Previous studies have focused on $PM_{2.5}$; however, due to the rising interest in PM1 and its health effects, attention should be brought to this particle fraction (Bari et al. 2015; Wang et al. 2021a). Further research and focus on exposure to PM_1 generated from ECIGs is needed to take into account the refractive index differences of ECIGs for optical monitors and dilution factors that

cause particle size misclassification for electrical mobility monitors. In addition, the study illustrates that the pDR, with the built-in filter that can be used for gravimetric analysis, has better performance and is a better solution for ECIG exposure monitoring than the SidePak. However, the pDR can only measure one particle size during operation, compared to the MiniWRAS that can measure different particle sizes and provide number concentration and aerosol size distribution. Therefore, given the price differences, the pDR is a better solution as a photometer, but the MiniWRAS is a comprehensive mobile solution given the price range is not an obstacle, and the aerosol concentrations are not considerably higher. The SidePak performs well and maybe a more cost-effective for researchers looking to monitor secondhand ECIG exposures in real-world settings.

Conflict of interest

Eric Soule is named on a patent for a device that determines electronic cigarette device and liquid characteristics.

Data availability statement

The datasets generated from the current study are available from the corresponding author on reasonable request.

Acknowledgments

The authors would like to thank Dr. Timothy Wright, formerly of North Carolina State University, for his help during this study

Funding

This research is supported by grant number R15ES032138 from the National Institute on Environmental Health Sciences of the National Institutes of Health. Part of E.S.'s efforts is also supported by grant numbers U54DA036105 from the National Institute on Drug Abuse and R21CA239188 from the National Cancer Institute of the National Institutes of Health and the Center for Tobacco Products (CTP) of the U.S. Food and Drug Administration. The content is solely the responsibility of the authors and does not necessarily represent the views of the NIH or the FDA.

ORCID

Sinan Sousan http://orcid.org/0000-0001-5524-6911
Eric Soule http://orcid.org/0000-0003-2740-5633

References

Ballbè, M., J. M. Martínez-Sánchez, X. Sureda, M. Fu, R. Pérez-Ortuño, J. A. Pascual, E. Saltó, and E. Fernández. 2014. Cigarettes vs. E-cigarettes: Passive exposure at home measured by means of airborne marker and biomarkers. *Environ. Res.* 135:76–80. doi:10.1016/j.envres.2014.09.005.

Bari, M. A., W. B. Kindzierski, L. A. Wallace, A. J. Wheeler, M. MacNeill, and M.-È. Héroux. 2015. Indoor and outdoor levels and sources of submicron particles (pm1) at homes in edmonton, canada. *Environ. Sci. Technol.* 49 (11):6419–29. doi:10.1021/acs.est.5b01173.

Breland, A., E. Soule, A. Lopez, C. Ramôa, A. El-Hellani, and T. Eissenberg. 2017. Electronic cigarettes: What are they and what do they do? *Ann N Y Acad Sci* 1394 (1):5–30. doi:10.1111/nyas.12977.

Burkart, J., G. Steiner, G. Reischl, H. Moshammer, M. Neuberger, and R. Hitzenberger. 2010. Characterizing the performance of two optical particle counters (grimm opc1.108 and opc1.109) under urban aerosol conditions. *J. Aerosol Sci.* 41 (10):953–62. doi:10.1016/j.jaerosci.2010.07.007.

Carwile, J. L., A. F. Fleisch, K. Young, and K. A. Ahrens. 2019. Electronic cigarette use in us households with children: The "new" secondhand Smoke. *JAMA Pediatr.* 173 (7):693–5. doi:10.1001/jamapediatrics.2019.1139.

Chen, R., A. Aherrera, C. Isichei, P. Olmedo, S. Jarmul, J. E. Cohen, A. Navas-Acien, and A. M. Rule. 2018. Assessment of indoor air quality at an electronic cigarette (vaping) convention. *J. Expo. Sci. Environ. Epidemiol.* 28 (6):522–9. doi:10.1038/s41370-017-0005-x.

Chen, G., S. Li, Y. Zhang, W. Zhang, D. Li, X. Wei, Y. He, M. L. Bell, G. Williams, G. B. Marks, et al. 2017. Effects of ambient pm1 air pollution on daily emergency hospital visits in china: An epidemiological study. *The Lancet Planetary Health* 1 (6):e221–e229. doi:10.1016/S2542-5196(17)30100-6.

Choi, H. S., Y. Ashitate, J. H. Lee, S. H. Kim, A. Matsui, N. Insin, M. G. Bawendi, M. Semmler-Behnke, J. V. Frangioni, and A. Tsuda. 2010. Rapid translocation of nanoparticles from the lung airspaces to the body. *Nat. Biotechnol.* 28 (12):1300–3. doi:10.1038/nbt.1696.

Czogala, J., M. L. Goniewicz, B. Fidelus, W. Zielinska-Danch, M. J. Travers, and A. Sobczak. 2014. Secondhand exposure to vapors from electronic cigarettes. *Nicotine Tob. Res.* 16 (6):655–62. doi:10.1093/ntr/ntt203.

David, G., E. A. Parmentier, I. Taurino, and R. Signorell. 2020. Tracing the composition of single e-cigarette aerosol droplets in situ by laser-trapping and raman scattering. *Sci. Rep.* 10 (1):7929 doi:10.1038/s41598-020-64886-5.

El-Hage, R., A. El-Hellani, C. Haddad, R. Salman, S. Talih, A. Shihadeh, T. Eissenberg, and N. Aoun Saliba. 2019. Toxic emissions resulting from sucralose added to electronic cigarette liquids. *Aerosol Sci. Technol.* 53 (10):1197–203. doi:10.1080/02786826.2019.1645294.

EPA. 1990. Criteria air pollutants: Naaqs table. Accessed March 2021. https://www.Epa.Gov/criteria-air-pollutants/naaqs-table.

EPA2021. Indoor air quality (iaq), indoor particulate matter. Accessed july 2021 https://www.Epa.Gov/indoor-air-quality-iaq/indoor-particulate-matter].

Fernández, E., M. Ballbè, X. Sureda, M. Fu, E. Saltó, and J. M. Martínez-Sánchez. 2015. Particulate matter from electronic cigarettes and conventional cigarettes: A systematic review and observational study. *Curr. Environ. Health Rep.* 2 (4):423–9. doi:10.1007/s40572-015-0072-x.

Flora, J. W., N. Meruva, C. B. Huang, C. T. Wilkinson, R. Ballentine, D. C. Smith, M. S. Werley, and W. J. McKinney. 2016. Characterization of potential impurities and degradation products in electronic cigarette formulations and aerosols. *Regul. Toxicol. Pharmacol.* 74:1–11. doi:10.1016/j.yrtph.2015.11.009.

Gentzke, A. S., T. W. Wang, K. L. Marynak, K. F. Trivers, and B. A. King. 2019. Exposure to secondhand smoke and secondhand e-cigarette aerosol among middle and high school students. *Prev. Chronic Dis.* 16:E42–E42. doi:10.5888/pcd16.180531.

Goniewicz, M. L., J. Knysak, M. Gawron, L. Kosmider, A. Sobczak, J. Kurek, A. Prokopowicz, M. Jablonska-Czapla, C. Rosik-Dulewska, C. Havel, et al. 2014. Levels of selected carcinogens and toxicants in vapour from electronic cigarettes. *Tob. Control.* 23 (2):133–9. doi:10.1136/tobaccocontrol-2012-050859.

Goniewicz, M. L., and L. Lee. 2015. Electronic cigarettes are a source of thirdhand exposure to nicotine. *Nicotine Tob. Res.* 17 (2):256–8. doi:10.1093/ntr/ntu152.

GRIMM. 2010. Aerosol spectrometer and dust monitor, series 1.108 and 1.109 Accessed January 2022. http://cires1.colorado.edu/jimenez-group/Manuals/Grimm_OPC_Manual.pdf.

Hiler, M., N. Karaoghlanian, S. Talih, S. Maloney, A. Breland, A. Shihadeh, and T. Eissenberg. 2020. Effects of electronic cigarette heating coil resistance and liquid nicotine concentration on user nicotine delivery, heart rate, subjective effects, puff topography, and liquid consumption. *Exp. Clin. Psychopharmacol.* 28 (5):527–39. doi:10.1037/pha0000337.

Hinds, W. C. 1999. *Aerosol technology: Properties, behavior, and measurement of airborne particles.* 2nd ed. New York: Wiley-Interscience.

Hutzler, C., M. Paschke, S. Kruschinski, F. Henkler, J. Hahn, and A. Luch. 2014. Chemical hazards present in liquids and vapors of electronic cigarettes. *Arch. Toxicol.* 88 (7):1295–308. doi:10.1007/s00204-014-1294-7.

Hyde, 2021. Hyde electronic cigarettes disposable products. Accessed July 2021. http://hydedisposables.Com/.

Ingebrethsen, B. J., S. K. Cole, and S. L. Alderman. 2012. Electronic cigarette aerosol particle size distribution measurements. *Inhal. Toxicol.* 24 (14):976–84. doi:10.3109/08958378.2012.744781.

Jarrell, Z. R., M. R. Smith, X. He, M. Orr, D. P. Jones, and Y.-M. Go. 2021. Firsthand and secondhand exposure levels of maltol-flavored electronic nicotine delivery system vapors disrupt amino acid metabolism. *Toxicol. Sci.* 182 (1):70–81. doi:10.1093/toxsci/kfab051.

Jensen, R. P., W. Luo, J. F. Pankow, R. M. Strongin, and D. H. Peyton. 2015. Hidden formaldehyde in e-cigarette aerosols. *N. Engl. J. Med.* 372 (4):392–4. doi:10.1056/NEJMc1413069.

Jiang, R.-T., V. Acevedo-Bolton, K.-C. Cheng, N. E. Klepeis, W. R. Ott, and L. M. Hildemann. 2011. Determination of response of real-time sidepak am510 monitor to secondhand smoke, other common indoor aerosols, and outdoor aerosol. *J. Environ. Monit.* 13 (6):1695–702. doi:10.1039/c0em00732c.

JUUL. 2021. Learn about the ingredients in juulpods. Accessed July 2021. https://www.Juul.Com/learn/pods.

Kane, D. B., and W. Li. 2021. Particle size measurement of electronic cigarette aerosol with a cascade impactor. *Aerosol Sci. Technol.* 55 (2):205–14. doi:10.1080/02786826.2020.1849536.

Klepeis, N. E., W. R. Ott, and P. Switzer. 2007. Real-time measurement of outdoor tobacco smoke particles. *J. Air Waste Manag. Assoc.* 57 (5):522–34. doi:10.3155/1047-3289.57.5.522.

Kosmider, L., A. Sobczak, M. Fik, J. Knysak, M. Zaciera, J. Kurek, and M. L. Goniewicz. 2014. Carbonyl compounds in electronic cigarette vapors: Effects of nicotine solvent and battery output voltage. *Nicotine Tob. Res.* 16 (10):1319–26. doi:10.1093/ntr/ntu078.

Liu, Y., and P. H. Daum. 2000. The effect of refractive index on size distributions and light scattering coefficients derived from optical particle counters. *J. Aerosol Sci.* 31 (8):945–57. doi:10.1016/S0021-8502(99)00573-X.

Logue, J. M., M. Sleiman, V. N. Montesinos, M. L. Russell, M. I. Litter, N. L. Benowitz, L. A. Gundel, and H. Destaillats. 2017. Emissions from electronic cigarettes: Assessing vapers' intake of toxic compounds, secondhand exposures, and the associated health impacts. *Environ. Sci. Technol.* 51 (16):9271–9. doi:10.1021/acs.est.7b00710.

McGrath-Morrow, S. A., J. Gorzkowski, J. A. Groner, A. M. Rule, K. Wilson, S. E. Tanski, J. M. Collaco, and J. D. Klein. 2020. The effects of nicotine on development. *Pediatrics* 145 (3):1–12. doi:10.1542/peds.2019-1346.

Melstrom, P., B. Koszowski, M. H. Thanner, E. Hoh, B. King, R. Bunnell, and T. McAfee. 2017. Measuring pm2.5, ultrafine particles, nicotine air and wipe samples following the use of electronic cigarettes. *Nicotine Tobacco Re.* 19 (9):1055–61. doi:10.1093/ntr/ntx058.

NJOY. 2021. Njoy electronic cigarette products. Accessed July 2021. https://njoy.Com/us/shop/daily/njoy-daily-menthol/].

Olegario, J. M., S. Regmi, and S. Sousan. 2021. Evaluation of low-cost optical particle counters for agricultural exposure measurements. *Applied Engineering in Agriculture* 37 (1):113–22. doi:10.13031/aea.14091.

PerfectVap. 2021. Menthol melon ingredients for box mod devices. Accessed July 2021: https://perfectvape.Com/naked-100-premium-e-liquid-60ml/.

Peters, T. M., H. Chein, D. A. Lundgren, and P. B. Keady. 1993. Comparison and combination of aerosol size distributions measured with a low pressure impactor, differential mobility particle sizer, electrical aerosol analyzer, and aerodynamic particle sizer. *Aerosol Sci. Technol.* 19 (3):396–405. doi:10.1080/02786829308959647.

Protano, C., M. Manigrasso, P. Avino, and M. Vitali. 2017. Second-hand smoke generated by combustion and electronic smoking devices used in real scenarios: Ultrafine particle pollution and age-related dose assessment. *Environ. Int.* 107:190–5. doi:10.1016/j.envint.2017.07.014.

Rosenberg, P. D., A. R. Dean, P. I. Williams, J. R. Dorsey, A. Minikin, M. A. Pickering, and A. Petzold. 2012. Particle sizing calibration with refractive index correction for light scattering optical particle counters and impacts upon pcasp and cdp data collected during the fennec

campaign. *Atmos. Meas. Tech.* 5 (5):1147–63. doi:10.5194/amt-5-1147-2012.

Schober, W., L. Fembacher, A. Frenzen, and H. Fromme. 2019. Passive exposure to pollutants from conventional cigarettes and new electronic smoking devices (iqos, e-cigarette) in passenger cars. *Int. J. Hyg. Environ. Health.* 222 (3):486–93. doi:10.1016/j.ijheh.2019.01.003.

Schober, W., K. Szendrei, W. Matzen, H. Osiander-Fuchs, D. Heitmann, T. Schettgen, R. A. Jörres, and H. Fromme. 2014. Use of electronic cigarettes (e-cigarettes) impairs indoor air quality and increases feno levels of e-cigarette consumers. *Int. J. Hyg. Environ. Health.* 217 (6):628–37. doi:10.1016/j.ijheh.2013.11.003.

Schripp, T., D. Markewitz, E. Uhde, and T. Salthammer. 2013. Does e-cigarette consumption cause passive vaping? *Indoor Air.* 23 (1):25–31. doi:10.1111/j.1600-0668.2012.00792.x.

Sleiman, M., J. M. Logue, V. N. Montesinos, M. L. Russell, M. I. Litter, L. A. Gundel, and H. Destaillats. 2016. Emissions from electronic cigarettes: Key parameters affecting the release of harmful chemicals. *Environ. Sci. Technol.* 50 (17):9644–51. doi:10.1021/acs.est.6b01741.

Soule, E. K., S. F. Maloney, T. R. Spindle, A. K. Rudy, M. M. Hiler, and C. O. Cobb. 2017. Electronic cigarette use and indoor air quality in a natural setting. *Tob. Control.* 26 (1):109–12. doi:10.1136/tobaccocontrol-2015-052772.

Sousan, S.,. A. Gray, C. Zuidema, L. Stebounova, G. Thomas, K. Koehler, and T. Peters. 2018. Sensor selection to improve estimates of particulate matter concentration from a low-cost network. *Sensors* 18 (9):3008. doi:10.3390/s18093008.

Sousan, S.,. K. Koehler, L. Hallett, and T. M. Peters. 2016a. Evaluation of the alphasense optical particle counter (opc-n2) and the GRIMM portable aerosol spectrometer (pas-1.108). *Aerosol Sci. Technol.* 50 (12):1352–65. doi:10.1080/02786826.2016.1232859.

Sousan, S.,. K. Koehler, G. Thomas, J. H. Park, M. Hillman, A. Halterman, and T. M. Peters. 2016b. Inter-comparison of low-cost sensors for measuring the mass concentration of occupational aerosols. *Aerosol Sci. Technol.* 50 (5):462–73. doi:10.1080/02786826.2016.1162901.

Sousan, S.,. S. Regmi, and Y. M. Park. 2021. Laboratory evaluation of low-cost optical particle counters for environmental and occupational exposures. *Sensors* 21 (12):4146. doi:10.3390/s21124146.

Sundahl, M., E. Berg, and M. Svensson. 2017. Aerodynamic particle size distribution and dynamic properties in aerosols from electronic cigarettes. *J. Aerosol Sci.* 103:141–50. doi:10.1016/j.jaerosci.2016.10.009.

Talih, S., Z. Balhas, R. Salman, R. El-Hage, N. Karaoghlanian, A. El-Hellani, M. Baassiri, E. Jaroudi, T. Eissenberg, N. Saliba, et al. 2017. Transport phenomena governing nicotine emissions from electronic cigarettes: Model formulation and experimental investigation. *Aerosol Sci. Technol.* 51 (1):1–11. doi:10.1080/02786826.2016.1257853.

Talih, S., R. Salman, R. El-Hage, E. Karam, S. Salam, N. Karaoghlanian, A. El-Hellani, N. Saliba, and A. Shihadeh. 2020. A comparison of the electrical characteristics, liquid composition, and toxicant emissions of juul USA and juul uk e-cigarettes. *Sci. Rep.* 10 (1):7322 doi:10.1038/s41598-020-64414-5.

Talih, S., R. Salman, E. Soule, R. El-Hage, E. Karam, N. Karaoghlanian, A. El-Hellani, N. Saliba, and A. Shihadeh. 2021. Electrical features, liquid composition and toxicant emissions from 'pod-mod'-like disposable electronic cigarettes. *Tob. Control* doi:10.1136/tobaccocontrol-2020-056362.

ThermoFisherScientific. 2010. Mie adr-1500 instruction manual. Particulate monitor, air quality instruments. Par number 108836-00. Franklin, ma.

VAPING. 2021. Drag 2 refresh edition kit. Accessed July 2021. https://vaping.Com/voopoo-drag-2-kit.

Vargas-Rivera, M., M. Ebrahimi Kalan, M. Ward-Peterson, O. Osibogun, W. Li, D. Brown, T. Eissenberg, and W. Maziak. 2021. Effect of flavour manipulation on ends (juul) users' experiences, puffing behaviour and nicotine exposure among us college students. *Tob. Control* 30 (4):399–404. doi:10.1136/tobaccocontrol-2019-055551.

Visser, W. F., W. N. Klerx, H. Cremers, R. Ramlal, P. L. Schwillens, and R. Talhout. 2019. The health risks of electronic cigarette use to bystanders. *Ijerph.* 16 (9):1525. doi:10.3390/ijerph16091525.

Volesky, K. D., A. Maki, C. Scherf, L. Watson, K. Van Ryswyk, B. Fraser, S. A. Weichenthal, E. Cassol, and P. J. Villeneuve. 2018. The influence of three e-cigarette models on indoor fine and ultrafine particulate matter concentrations under real-world conditions. *Environ. Pollut.* 243 (Pt B):882–9. doi:10.1016/j.envpol.2018.08.069.

Wang, Z., L. Calderón, A. P. Patton, M. Sorensen Allacci, J. Senick, R. Wener, C. J. Andrews, and G. Mainelis. 2016. Comparison of real-time instruments and gravimetric method when measuring particulate matter in a residential building. *J. Air Waste Manag. Assoc.* 66 (11):1109–20. doi:10.1080/10962247.2016.1201022.

Wang, H., F. Lu, M. Guo, W. Fan, W. Ji, and Z. Dong. 2021a. Associations between pm1 exposure and daily emergency department visits in 19 hospitals, Beijing. *Sci. Total Environ.* 755:142507. doi:10.1016/j.scitotenv.2020.142507.

Wang, X., Z. Xu, H. Su, H. C. Ho, Y. Song, H. Zheng, M. Z. Hossain, M. A. Khan, D. Bogale, H. Zhang, et al. 2021b. Ambient particulate matter (pm1, pm2.5, pm10) and childhood pneumonia: The smaller particle, the greater short-term impact? *Sci. Total Environ.* 772:145509. doi:10.1016/j.scitotenv.2021.145509.

WHO. 2010. Who guidelines for indoor air quality selected pollutants. Accessed July 2021. https://www.Euro.Who.Int/__data/assets/pdf_file/0009/128169/e94535.Pdf

WHO. 2018. Ambient (outdoor) air pollution. Accessed July 2021. https://www.Who.Int/news-room/fact-sheets/detail/ambient-(outdoor)-air-quality-and-health.

Williams, M., K. Bozhilov, S. Ghai, and P. Talbot. 2017. Elements including metals in the atomizer and aerosol of disposable electronic cigarettes and electronic hookahs. *PloS One.* 12 (4):e0175430. doi:10.1371/journal.pone.0175430.

Williams, M., A. Villarreal, K. Bozhilov, S. Lin, and P. Talbot. 2013. Metal and silicate particles including nanoparticles are present in electronic cigarette cartomizer fluid and aerosol. *PloS One* 8 (3):e57987. doi:10.1371/journal.pone.0057987.